

3D Printing with Flying Robots

Graham Hunt, Faidon Mitzalis, Talib Alhinai, Paul A Hooper, Mirko Kovac¹

Abstract— Extensive work has been devoted recently to the development of 3D printing or additive layer manufacturing technologies, as well as to the field of flying robots. However, to the best of the authors' knowledge, no robotic prototype has been presented so far that combines additive layer manufacturing techniques with aerial robotics. In this paper, we examine the feasibility of such a hybrid approach and present the design and characterisation of an aerial 3D printer; a flying robot capable of depositing polyurethane expanding foam in mid-flight. We evaluate various printing materials and describe the design and integration of a lightweight printing module onto a quadcopter, as well as discuss the limitations and opportunities for aerial construction with flying robots using the developed technologies. Potential applications include ad-hoc construction of first response structures in search and rescue scenarios, printing structures to bridge gaps in discontinuous terrain, and repairing damaged surfaces in areas that are inaccessible by ground-based robots.*

I. INTRODUCTION

3D printing or additive manufacturing has seen great development in recent years and has become an established method of manufacturing with many applications. However, 3D printing typically requires a fixed size printer with a limited printing envelope. The size of the parts produced are therefore limited by the size of the printer itself and in most cases scaling up the printer is impractical and costly.

This paper examines the feasibility of an aerial 3D printing robot (shown in Figure 1) that overcomes restrictions in the size of the printed structure and allows a significant amount of flexibility in printing location. The material deposition is performed by a quadcopter carrying an on-board printing system and depositing material whilst in motion. This allows it to print three dimensional structures in areas normally inaccessible by ground or climbing robots with a variety of maintenance and repair applications.

The use of mobile robots that deposit material is a new area of research and, to the best of our knowledge, a flying 3D printing robot has not been presented so far. However, extensive research has been carried out on the two parts of the system individually, mobile airborne robots and material deposition systems for 3D printers.

One approach of additive manufacturing techniques best suited for the needs of the project is fused deposition modelling (FDM) [1]. FDM uses extruded thermoplastic or wax from a heatable extrusion head to trace out the solid areas of the physical models. The extrusion head can move on the horizontal plane depositing very thin beads of molten material on a heated platform. Vertical motion of

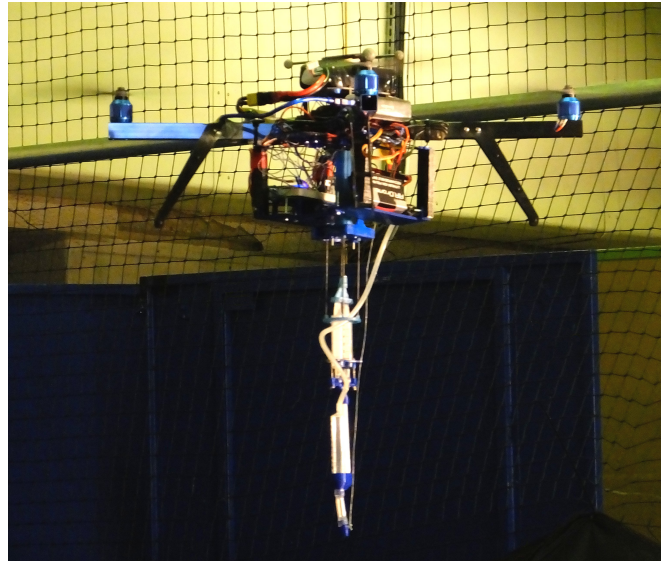


Fig. 1. Aerial 3D printer, quadcopter with integrated printing module in orientation ready for printing

the platform allows subsequent layers to be printed using the same procedure [2]. Unlike other methods, such as stereolithography or selective laser sintering, FDM does not require a pool of material and is therefore more suitable for unrestricted deposition in three-dimensional space.

MAVs (Micro Air Vehicle), such as quadcopters, allow for accurate positioning and flexibility of motion in all three directions to facilitate material deposition. The current state in mobility and control of quadcopters shows that advanced flight and control has been achieved [3]–[7], and the navigation and localisation can be achieved with current technology [8]–[11].

In the pursuit of large scale automated construction, a promising example of an alternative 3D printer has been developed by [12], where one of the solutions involved depositing concrete using a gantry robot. A second approach to create mobile construction robots is a swarm of remote controlled ground vehicle developed by [13, 14], able to construct a ramp using various amorphous materials. Other examples of robotic fabrication using amorphous materials includes the use of thermoplastic adhesives to build robotic building tools [15] and spider inspired drag lines [16]. Further examples of automated construction involved assembling prefabricated components using quadcopters [17, 18].

In comparison to existing systems, the solution we propose combines a trajectory guided quadcopter with an on-board printing system to simulate the printing head of a

*See video attachment

This work was done at the Aerial Robotics Lab, Imperial College London

¹Corresponding author: m.kovac@imperial.ac.uk

conventional 3D printer. The quadcopter allows flexibility in positioning of the printing nozzle in all three dimensions. A material of high viscosity is required for deposition in order to retain the shape followed by the moving robot. The geometry of the printed structure can be altered by controlling the path and dynamics of the robot and an advantage of an aerial robot, in contrast to a ground system, is that it can reach high elevations easily and build 3D structures in inaccessible or hazardous areas.

II. PRINTING MATERIAL

A promising printing method to integrate on a flying platform is a system that resembles Fused Deposition Modelling techniques that are used in conventional 3D printers. The material is deposited in a very viscous liquid form and cures upon extrusion from the printing nozzle. Using this technique the printed geometry depends on the path followed by the printing nozzle. Hence the robot itself, and the flow rate of the material can control the printed geometry. A major challenge is to choose a suitable material for successful integration on the flying robot.

A. Material Selection

The feasibility of a controllable, lightweight printing system largely depends on the material used for printing and the main properties that were considered in selection are listed below.

- 1) Density of the printing material
- 2) Curing time
- 3) Material strength after solidification
- 4) Expansion of the material after curing
- 5) Cost

Based on a comparison (Table I) we concluded that two part polyurethane (PU) foam is the best solution, providing a large volume expansion in a short time scale. PU foam consists of two components, component one contains polyetherols, flame-retardant, silicone, catalyst and blowing agents (Chemical A) and the second component is a diisocyanato diphenylmethane (MDI) based composition (Chemical B). The main advantage of two part polyurethane expanding foam is the very large expansion during solidification, approximately 25 times its initial volume. In this way a small volume of material can be carried on the flying platform, expanding to a considerably larger volume of printed structure after deposition. Additionally, using two part liquid solutions, the two chemicals are stored separately which ensures that the material is in a non-reacting state before the printing process is initiated. Furthermore, a refilling system can potentially be achieved by pumping liquid inside the two containers, a process which could be performed autonomously by the robot. The material is also self-adhesive and can be applied to a wide variety of surfaces. A significant challenge using the two part polyurethane foam is achieving high quality mixing and a high viscosity solution on-board the robot with a lightweight printing system.

B. Material Testing

We performed preliminary testing of the material to determine the design requirements of the printing system for high quality printing. The main parameter was the time required for the two liquids to react and start producing foam.

A static mixing nozzle was used to mix the two chemicals. In the first tests, the two chemicals were well mixed when leaving the nozzle but the mixture was still in liquid form when it was deposited. A more viscous, foam form was required for printing to avoid the material spreading on the surface, producing undesirable results. The module design was altered to introduce a reaction chamber after the mixing nozzle, where the two chemicals are held until they fully react and produce foam. Material deposition starts after the foam starts forming, when the material is in a very viscous state allowing for the shape to be maintained after printing.

To determine the required reaction time we deposited foam samples with a time of 45s, 60s, 75s and 90s on a 30° inclined slope and its shape changed until full hardening (Figure 2).

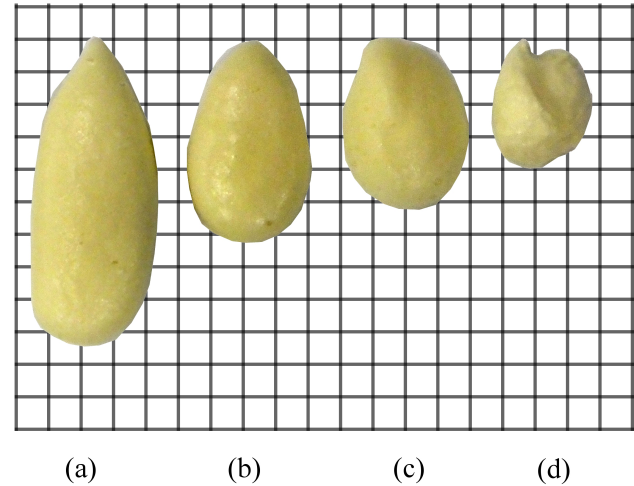


Fig. 2. Examples (a) to (d) show a foam deposit after increasing reaction time. The viscosity after a reaction time of 45s is too inviscid for deposition. The limiting time was observed to be 90s, before the foam hardened too much for deposition (a): 45s (b): 60s (c): 75s (d): 90s Grid spacing: 10mm

III. DESIGN

The design method followed was to divide the system into the printing module and the mobility platform. The printing module delivers the material in a highly viscous form and deposits the material at the position of the printing nozzle. Using the quadcopter platform the robot can move to the required location and follow the path required to form the intended geometry by depositing material along its way.

A. Printing System

From the materials considered, two part polyurethane expanding foam was chosen as the most appropriate material for the application. The processes required by the printing system for polyurethane foam are, storing the two chemicals

TABLE I
MATERIAL COMPARISON

Material	Density kg/m ³ (after expansion)	Expansion	Curing Time	Heating Required?
Single Part Polyurethane Foam	3	24 times	~4 hours	No
Two Part Polyurethane Foam	48-50	~25 times	15 mins	No
Thermoplastics (ABS)	1,042	~1 times	5 s	Yes
Two Part Epoxy Adhesive	250	1 times	24 hours	No
Hot Glue	960	1 times	1 min	Yes

in separate containers, delivering and mixing the chemicals on-board the quadcopter, and finally depositing the material through a printing nozzle. The process and timings are summarised in Figure 3.

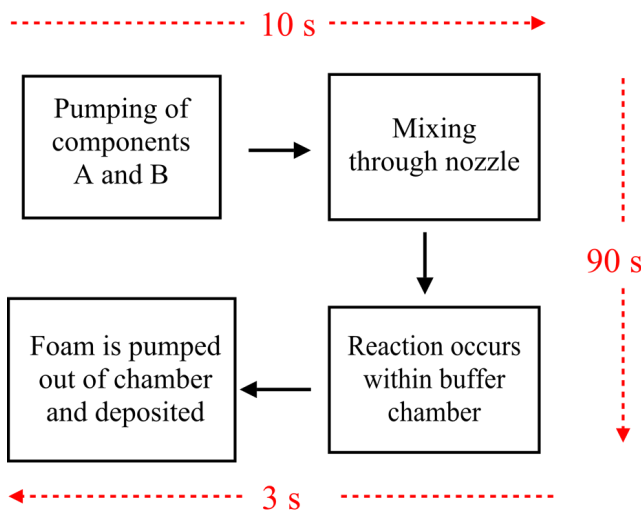


Fig. 3. Schematic showing order and allocated times (in red) of each process which occurs within the printing nozzle. The printing operation requires 103 seconds to complete.

A major design criterion of the printing system was the mass of the system. To achieve continuous steady flight, the maximum payload of the quadcopter is approximately 500g. Additionally, ease of manufacture was a key aspect in the design as many parts of the system had to be replaceable to avoid clogging, especially in places where the mixture could potentially solidify prior to deposition. The main design criteria are summarised in Table II, focusing on low cost, robustness and low weight.

TABLE II
DESIGN CRITERIA FOR PRINTING SYSTEM

Criterion	Aim	Importance (1 to 5)
Total Mass	<130 grams	5
Cost of Materials	Less than £5 (excluding actuators)	2
Ease of Manufacture	Use standard parts	4
Compact	Fit on quadcopter base	5
High Toughness	Limit damage upon impact	2

The assembly of all the components of the printing system

is shown in Figure 4. The major component assemblies within the module are discussed individually in the following sections.

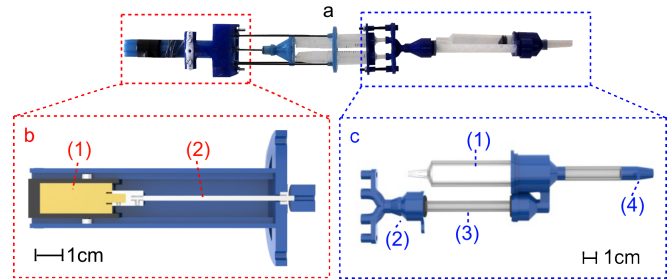


Fig. 4. Complete printing module with a CAD breakdown of components. a: Printing module b(1): Micro geared motor b(2): M2 Lead screw c(1): Buffer chamber for chemical reaction process c(2): Customized chemical mixing junction, c(3): Mixing nozzle, c(4):Printing Nozzle

1) *Delivery System:* The two chemicals are stored in two separate containers. The containers used are two 5mL syringes which can also be used to pump the liquid out using the plunger. Manufacturing modifications have to be made to the syringes used in the system in order to reduce weight. The configuration of the delivery actuator is shown in Figure 5.

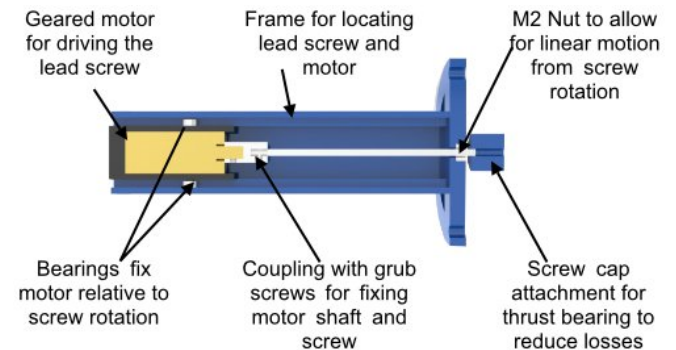


Fig. 5. CAD render cross-section of delivery actuator for mixing chemicals A and B. A lead screw design is utilised to provide linear actuation of the two storage container plungers.

Essential for accomplishing good mixing quality is to ensure that the flows of Chemical A and Chemical B are equal, as a consistent 1:1 mixing ratio is required. To achieve this a lead screw design was utilised to provide the linear

TABLE III
WEIGHT BUDGET

Part	Weight (g)	Manufacturing
Delivery Module		
Micro geared motor	10	Commercial Component
M2 Lead screw	2	Commercial Component
Miniature bearings (2x)	1	Commercial Components
Housing	11	3D Printed PLA
Component Syringe (2x)	5	Commercial Component
Lead screw attachment	2	3D Printed PLA
Disposable Components		
Mixing Nozzle	3	Commercial Component
Mixing Junction	3	3D Printed PLA
Foam Junction	5	3D Printed PLA
Reaction Chamber	4	Commercial Component
Printing Nozzle	1	3D Printed PLA
Other		
Mounting rig and electronic components	157	-
Miscellaneous (Rubber tubing, thread, wiring)	28	-
Total	232	-

force to move the syringe plungers. The screw is driven by a motor and the power required for this motor is matched to the force required to move both container syringes. The two 5ml syringes are placed parallel and inline with the lead screw and the force is applied to both plungers equally. This is a powerful lightweight solution that ensures that the flows of the two chemicals are equal. The mass associated with each component is listed in Table III. This shows there is an additional 250g of capacity for increasing the chemical payload, from the current 5ml of each component ($\sim 10\text{g}$), with minor adjustments to the structural design.

2) *Mixing Components*: The two chemicals are mixed by joining the flows with a custom design Y-splitter and pumping them through a disposable mixing nozzle (Figure 6). The mixing nozzle is a static mixer, whose internal geometry enhances mixing of the two chemicals. At the exit of the mixing nozzle the two chemicals are fully mixed.

Testing showed that mixing of the two chemicals using the static mixer is satisfactory. However, the mixture is still in liquid form and not viscous enough for deposition. In that form the printing material would spread on the surface it is deposited on. To overcome this problem and produce the foam prior to deposition, more time is needed for the two chemicals to react.

3) *Reaction Chamber*: In order to provide more time for the two chemicals to react, the mixture is held in a reaction chamber until the mixture starts taking the required form. Material testing showed that approximately 90 seconds after the flow initiates the mixture is of an adequate viscosity for deposition. Until that time the mixture is held in the reaction chamber.

The reaction chamber is constructed from a 10 mL syringe, one side has two lines connected the inflow and outflow of the mixture. The other side is used to pressurise the syringe using an air pump. When foam starts forming and the material is ready for deposition, air is pressurised in the syringe so the material is pushed through the outflow to the

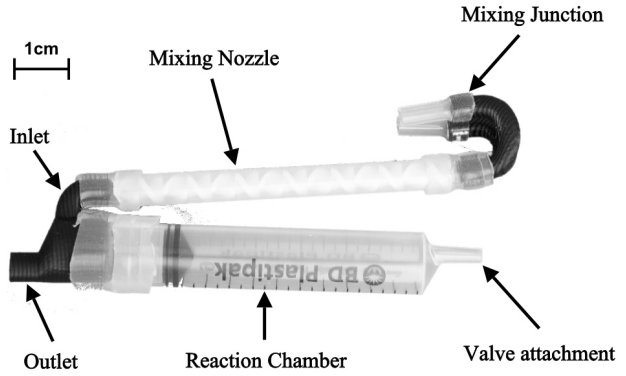


Fig. 6. Reaction Chamber plus the foam junction which leads to the printing nozzle. The foam junction also has an intake port through which mixed components are delivered from the mixing nozzle

printing nozzle. The reaction chamber is shown in Figure 6.

4) *Nozzle Valve*: A single valve is required on the printing nozzle to prevent outflow of the chemical mixture prior to complete mixing and reaction. Due to weight restrictions pinch valves, which would be suitable for the application, could not be used. Hence, we designed a custom valve system to block and release the flow. The valve system uses a servo to pull and bend the silicon tubing to block the flow of air and foam by forming a seal against the printing module support.

5) *Printing Nozzle*: The last component of the printing system is the printing nozzle. Various shapes can be used for the printing nozzle depending on the required shape of the foam. We designed a simple nozzle that ensures the material is deposited in a laminar fashion in order to optimise the accuracy of the final release of foam.

B. Aerial Platform

The printing system has been designed to be attached to the 3DR ArduCopter Quad. The quadcopter has an on-board processor (ArduPilot), three axes accelerometer, three axes magnetometers and speed controllers on all four brushless motors. For accurate localisation in the flight arena, we use a 3D motion tracking system with 16 Vicon T40 cameras [19]. A separate off-board controller uses the tracking coordinates from the Vicon system and transmits commands at a frequency of 50Hz to the on-board processor to control its position.

The flight stability and accuracy required is a major challenge, however the focus of this paper is on the automated foam deposition mechanism and not on the control of the platform. The underactuated nature of the quadcopter [20], the significant payload from the printing module ($\sim 300\text{g}$) and minor imbalances in mass distribution render the system challenging to control. For flight control, a cascaded PID controller was used [21] that is specifically developed for this platform. Accuracy within 10cm in all three translational directions was achieved, which was sufficient for successful printing results. Significant improvements in the results are expected if a more advanced controller is adopted such as

optic flow stability based flight control. Future work will address the integration of the presented printing module on a flying robot with on-board flight control and navigation that would not rely on a motion tracking environment.

Extensive testing of the system showed that the effects of the downwash and the distance from the ground do not significantly affect the precision of the print. The speed of deposition suggests that the entirety the print is within a small region even if the robot is drifting around the target position while depositing, this is shown in the video attached.

IV. INTEGRATION

The printing module must be integrated into the quadcopter system in a manner which is robust and does not compromise the performance of the robot.

A. Mounting

In order to mount the printing module on to the quadcopter a rig was designed (Figure 7). The rig has two main functions, firstly it acts to attach the printing module to the base of the robot. The rig is designed such that there is a clearance between the quadcopter's legs and the base of the module. This is intended to prevent any damage to the module during landing or in the event of unexpected failure during flight.

Secondly the rig also allows for the rotation of the printing module (Figure 8). This rotation is performed by a servo actuator fixed onto the mounting rig enabling vertical alignment during a printing operation. This orientation increases the robot's ground clearance during printing, reducing turbulent ground effects leading to improved deposition accuracy. Travelling to the print position and landing however is impractical with the module in this orientation, therefore the module is rotated to the horizontal, bringing it to a secure position before and after performing a print.

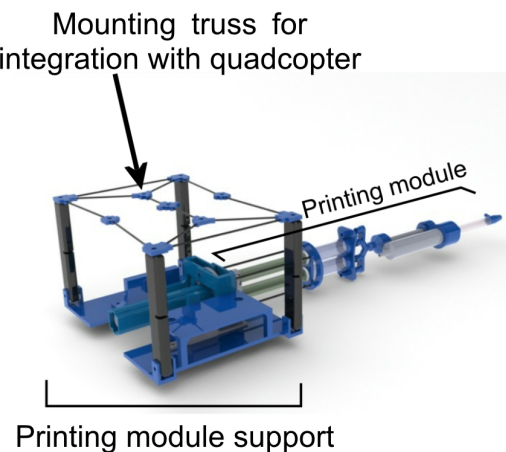


Fig. 7. CAD Model of printing module attached to mounting rig

B. Dynamic Coupling of the Combined System

The printing module represents a mass at a location displaced from the quadcopter centre of mass. This produces

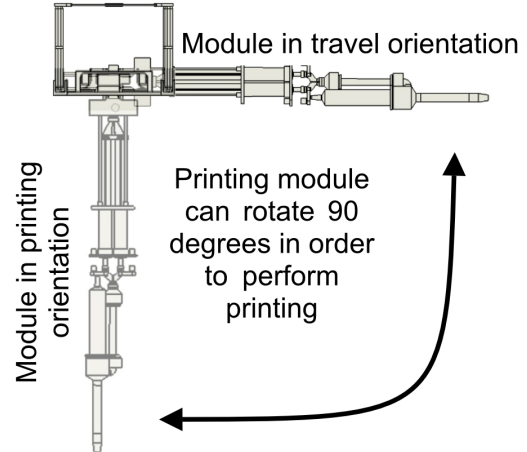


Fig. 8. The module is held vertically to perform a print operation and is held horizontally for travelling and landing

an imbalance in the system which the controller must continually account for. In addition to this, the movement of the printing arm from horizontal to vertical position, or vice versa, upsets the stability of the quadcopter during hover. The controller responds to this input and the response can be seen in the supplementary video. To account for this issue, printing is delayed until the controller has responded and the quadcopter is stable again within predefined limits. In the future a more advanced controller could be implemented to reduce the effect of on-board movements.

V. RESULTS

We demonstrated the feasibility of an aerial 3D printer by performing airborne depositions using predefined flight paths tracked via a 3D motion capture system. In this section, we present the results and performance characterisation of the printing mechanism and the integrated aerial 3D printer robot. Further, we describe two printing scenarios and discuss the opportunities and limitations of the developed aerial 3D printing technologies for construction with flying robots.

A. Scenario 1: Bridging gaps in terrains

This scenario illustrates gap filling properties of the 3D printing method. The experimental setup consists of two suspended aluminium beams of a width of 25 mm separated by an air gap of 18mm. This setup abstracts a crack that needs to be bonded by the 3D printing robot. We performed five consecutive static depositions: twice on each aluminium beam and a final fifth print to further reinforce the bridged gap. The air gap between the beams was bridged after the second deposition (Figure 9a). Transitioning this to an airborne solution is now only dependent on the quality of flight controller.

The two beams were connected by a polyurethane foam bridge of cross-sectional area 1300 mm^2 . To characterise the strength of the bridge, we used a multi-axis load cell to measure the force required for fracture. The maximum load recorded was 153.9 N, corresponding to a yield stress

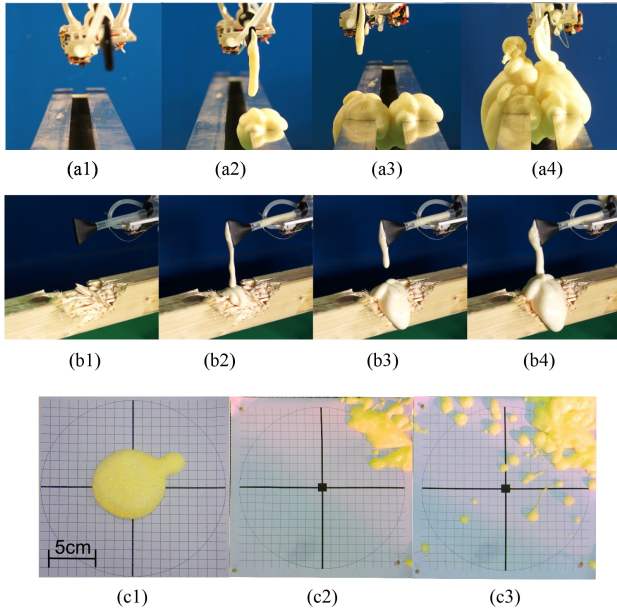


Fig. 9. (a1) - (a4) Shows the static deposition of material between an 18mm gap. (a4) shows the gap was successfully bridged; (b1) - (b4) shows the static deposition on a damaged wooden beam. (b4) shows how after a single print the damage has begun to be rectified by the robot; (c1) - (c3) shows comparison of static and airborne deposition accuracy. (c1) is a result whilst the robot is grounded, (c2) and (c3) shows a first and subsequent deposition whilst the robot is airborne.

of 118.0 kPa. Assuming that the tensile behaviour scales linearly, the same depth of foam printed along a metre long gap of width 18mm, the structure could withstand loading up to roughly 7.5 kN.

B. Scenario 2: Repairing damaged structures

As a demonstration of repairing damaged structures with the aerial 3D printing method developed in this paper, the second scenario consists of a damaged wooden beam and the foam printing mechanism that is held fixed above it. This experiment illustrates a potential scenario where a quadcopter prints foam over a damaged structure in access denied terrain to repair it. The results (Figure 9b) show that the foam is successfully used as filling material for the wooden beam. After hardening for five minutes it forms a rigid closed cell foam structure that adheres solidly to the wooden beam, indicating that the mechanism design and integration methods are successful as well as that polyurethane foam can be used as filling material for wooden structures. Again, achieving this result for an airborne deposition in the future would only be dependent on the establishing the required flight control.

C. Characterisation of deposition accuracy

Two successful prints are performed on a target (Figure 9c) and a compared to a print with the suspended mechanism. The results show that aerial 3D printing is achieved. The accuracy is shown to be highly dependent on the stability of the flight and is also affected by the downwash from

the propellers. Printing within a 10cm radius has been achieved (Figure 9c (2 & 3)) and with increasing flight stability, the accuracy of a static deposition described in the aforementioned scenarios can be approached (Figure 9c (1)).

VI. DISCUSSION

Possible related applications of the scenarios presented involve bridging air gaps to allow for land robots to overcome difficult terrain or to insulate and hold together overhead power lines during natural disasters. The range of applications of such an aerial 3D printer are very rich and span from local repair of damaged surfaces to construction of entire three dimensional structures. Combining the presented mechanism with swarm control and special navigation schemes, such as simultaneous localisation and mapping (SLAM), could allow for autonomous detection and repair using swarms of aerial printers. The main limitations are, low material capacity due to the relatively small payload capacity and limited battery life of the quadcopter, as well as inability to regulate and stop a printing cycle halfway through to move on and print at another location. Nevertheless, the current system proposes successful mechanical integration and methods for aerial printing with polyurethane foam and demonstrates a future for additive layer manufacturing in combination with aerial robots.

VII. CONCLUSION AND FUTURE WORK

In this paper, we presented the design and characterisation of an aerial 3D printer capable of depositing polyurethane foam to create structures in mid flight. Through two different scenarios, we demonstrate the capabilities and potential applications of this technique. Based on the characterisation and successful integration of a 3D printing module on a quadcopter, we conclude that aerial 3D printing is a promising new addition to the field of aerial construction. The major limitation of this construction technique is the limited payload of flying robots. Improved flight stability will allow more accurate deposition to facilitate printing of structures at tighter tolerances. Future work could therefore focus on multi-vehicle coordination to enable the construction of larger structures and automating the raw component refilling process to shorten intervals between successive prints. Adapting the system for different materials can further expand the applications of the system.

VIII. ACKNOWLEDGEMENT

The authors gratefully acknowledge the Department of Aeronautics at Imperial College London and The Engineering and Physical Sciences Research Council (EPSRC) for their support of this work. Any opinions, findings, and conclusions or recommendations in this material are those of the authors and do not necessarily reflect the views of the aforementioned entities. Talib Alhinai thanks the Abu Dhabi Investment Authority (ADIA) for financial support.

REFERENCES

- [1] Ian Gibson, David W Rosen, and Brent Stucker. *Additive manufacturing technologies: rapid prototyping to direct digital manufacturing*. Springer, 2010.
- [2] CJ Luis Perez. Analysis of the surface roughness and dimensional accuracy capability of fused deposition modelling processes. *International Journal of Production Research*, 40(12):2865–2881, 2002.
- [3] Sergei Lupashin, Angela Scholig, Michael Sherback, and Raffaello D’Andrea. A simple learning strategy for high-speed quadrocopter multi-flips. In *IEEE International Conference on Robotics and Automation (ICRA), 2010*, pages 1642–1648.
- [4] Aleksandr Kushleyev, Vijay Kumar, and Daniel Mellinger. Towards a swarm of agile micro quadrotors. In *Robotics: Science and Systems*, 2012.
- [5] Korbinian Schmid, Teodor Tomic, Felix Ruess, Heiko Hirschmuller, and Michael Suppa. Stereo vision based indoor/outdoor navigation for flying robots. In *IEEE/RSJ International Conference on Intelligent Robots and Systems (IROS), 2013*, pages 3955–3962.
- [6] Daniel Gurdan, Jan Stumpf, Michael Achtelik, K-M Doth, Gerd Hirzinger, and Daniela Rus. Energy-efficient autonomous four-rotor flying robot controlled at 1 khz. In *IEEE International Conference on Robotics and Automation, 2007*, pages 361–366.
- [7] Nathan Michael, Daniel Mellinger, Quentin Lindsey, and Vijay Kumar. The grasp multiple micro-uav testbed. *Robotics & Automation Magazine, IEEE*, 17(3):56–65, 2010.
- [8] Markus Hehn and Raffaello D’Andrea. Quadrocopter trajectory generation and control. In *IFAC World Congress*, pages 1485–1491, 2011.
- [9] Korbinian Schmid, Michael Suppa, and Darius Burschka. Towards Autonomous MAV Exploration in Cluttered Indoor and Outdoor Environments. *RSS 2013 Workshop on Resource-Efficient Integration of Perception, Control and Navigation for Micro Air Vehicles (MAVs)*, 2013.
- [10] Charles Richter, Adam Bry, and Nicholas Roy. Polynomial trajectory planning for quadrotor flight. In *International Conference on Robotics and Automation, 2013*.
- [11] Matthew Turpin, Kartik Mohta, Nathan Michael, and Vijay Kumar. Goal assignment and trajectory planning for large teams of aerial robots. In *Proc. Robotics: Science and Systems*, 2013.
- [12] Sungwoo Lim, Richard A. Buswell, Thanh T. Le, Simon A. Austin, Alistair GF Gibb, and Tony Thorpe. Developments in construction-scale additive manufacturing processes. *Automation in Construction*, 21:262–268, 2012.
- [13] Nils Napp, Olive R. Rappoli, Jessica M. Wu, and Radhika Nagpal. Materials and mechanisms for amorphous robotic construction. In *IEEE/RSJ International Conference on Intelligent Robots and Systems (IROS), 2012*, pages 4879–4885.
- [14] Justin Werfel, Kristin Peterson, and Radhika Nagpal. Designing collective behavior in a termite-inspired robot construction team. *Science Magazine*, 343:754–758, 2014.
- [15] Luzius Brodbeck, Liyu Wang, and Fumiya Iida. Robotic body extension based on hot melt adhesives. In *Robotics and Automation (ICRA), 2012 IEEE International Conference on*, pages 4322–4327. IEEE, 2012.
- [16] Liyu Wang, Utku Culha, and Fumiya Iida. A dragline-forming mobile robot inspired by spiders. *Bioinspiration and Biomimetics*, 9(1):016006, 2014.
- [17] Quentin Lindsey, Daniel Mellinger, and Vijay Kumar. Construction of cubic structures with quadrotor teams. *Robotics: Science and Systems*, 2011.
- [18] Jan Willmann, Federico Augugliaro, Thomas Cadalbert, Raffaello D’Andrea, Fabio Gramazio, and Matthias Kohler. Aerial robotic construction towards a new field of architectural research. *International journal of architectural computing*, 10(3):439–460, 2012.
- [19] Motion Systems Vicon. Vicon, August 2013.
- [20] Inkyu Sa and Peter Corke. System identification, estimation and control for a cost effective open-source quadcopter. In *IEEE International Conference on Robotics and Automation (ICRA), 2012*, pages 2202–2209.
- [21] Adam Braithwaite and Mirko Kovac. An extensible on-board flight control system for the arducopter platform. *In review*, 2014.